COBEM 2021 26th International Congress of Mechanical Engineering
November 22-26, 2021, Virtual Congress, Brazil
ABCM Associação Brasileira de Engenharia e Ciências Mecânicas

COB-2021-0489
DESIGN OF A TORQUE AND THRUST BIAXIAL SENSOR FOR PROPELLERS

Gabriel Pereira Gouveia da Silva
João Paulo Eguea
Fernando Martini Catalano
Universidade de São Paulo – Depto. Eng. Aeronáutica, Av. João Dagnone, 1100 – São Carlos – SP, 13563-120
gabriel.gouveia.silva@usp.br, joao.eguea@usp.br, catalano@sc.usp.br

Abstract. *The propulsive performance of a propeller is related to its capacity to generate more thrust with less torque, which can be measured with torque and thrust biaxial load cells. The work presented hereby refers to the design of aerodynamic balances for a distributed electric propulsion test rig. These balances were designed to provide an independent measurement of thrust and torque, with a linear response to the applied loads. The balances are composed of aluminum alloy blades, that are flexed by the axial displacement of their ends caused by the propeller thrust; and a cylindrical rod with a hollow section, that is more easily deformed by the propeller torque. These load cells were instrumented with linear strain gauges connected in a full-bridge for the measurement of thrust and fishbone strain gauges in a half-bridge for the measurement of torque. The load cells were simulated using finite element software and were manufactured in aluminum alloy through traditional and electrical discharge machining. The strain gauges have been installed and the balances will be calibrated with known loads. A measurement of the balance hysteresis will also be carried out. After the calibration process, the balances will be ready for use in the test rig.*

Keywords: *wind tunnel testing, aerodynamic balance, propeller test, propeller aerodynamics, load cell.*

1. INTRODUCTION

The emergence of urban air mobility aircraft has been driving a need for quieter and more efficient propellers (Kim *et al.*, 2018; International Civil Aviation Organization, 2019). These new propellers should be capable of obtaining an extra benefit from the aeropropulsive integration (Cole *et al.*, 2019). Thus, the relationships between the performance and acoustic parameters and the propellers' position, geometric and operational characteristics need to be known to the propeller designer. In this context, a test rig for distributed electric propulsion (DEP) was built at the Department of Aeronautical Engineering of the University of São Paulo (EESC-USP). It will be used to obtain an experimental database of propellers operating in DEP conditions. This database will improve the understanding of the interaction between propellers and wing and between adjacent propellers. It will also provide a means of validation for design tools for optimizing propellers for DEP.

The propulsive performance is related to the propeller capacity to generate more thrust with less torque and can be evaluated experimentally through measurements with torque and thrust biaxial load cells (Barlow *et al.*, 1999; Doebelin and Manik, 2007; Discetti and Ianiro, 2017). The characteristics required for the design of such load cells are:

- the presence of elements that deform preferably due to the applied thrust force, with negligible deformation due to the weight of the motor and the torque of the propeller, ensuring an independent measure of thrust;
- the presence of an element that deforms preferably due to the torque applied, with negligible deformation due to the weight of the motor and the thrust of the propeller, ensuring an independent measure of torque;
- a natural frequency of the first mode of vibration much higher than that expected for the rotational speeds of the tested propellers, ensuring that dynamic loads do not affect the static measurements and that the structure remains intact;
- compactness so that the installation of the balance does not significantly impact the aerodynamic performance of the DEP wing.

The work presented hereby refers to the conceptual design and finite element method (FEM) simulations of a propeller balance that complies with the requirements listed above. It was designed for the EESC-USP DEP test rig.

2. BALANCE DESIGN

The balance was designed to be made of aluminum alloy in order to be lightweight, flexible, and resistant. It is composed of aluminum alloy blades, that are flexed by the axial displacement of their ends caused by the propeller thrust (while being rigid to resist the bending caused by the propeller torque); and a cylindrical shaft with a hollow section, that is more easily deformed by the propeller torque between the fixation of the motor and the fixation of the load cell in the balance casing (Fig. 1). After the machining, these load cells were instrumented with linear strain gauges connected in a full-bridge for the measurement of thrust and shear strain gauges in a half-bridge for the measurement of torque. The load cells were simulated using finite element software and were manufactured in aluminum alloy through traditional and electrical discharge machining. The strain gauges have been installed and the balances will be calibrated with known loads. A measurement of the balance hysteresis will also be carried out. After the calibration process, the balances will be ready for use in the test rig.

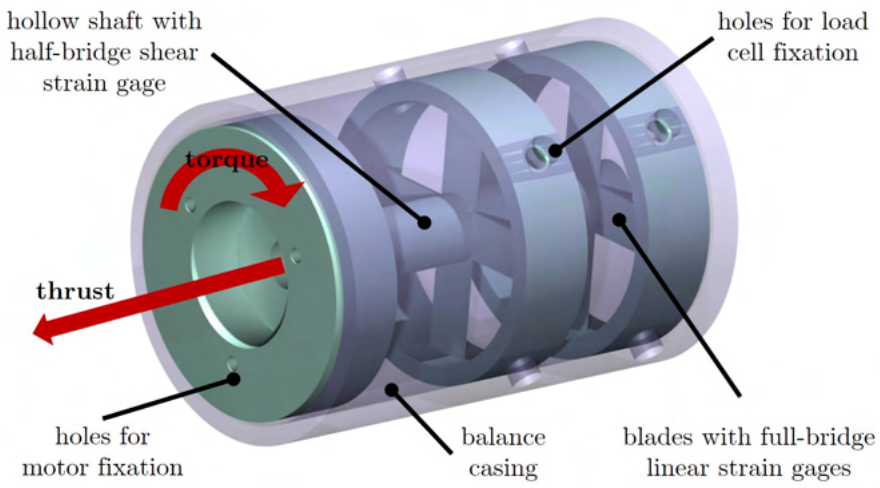

Figure 1. Details of the biaxial sensor designed by the authors to measure the thrust and torque of a propeller.

3. FEM SIMULATION SETUP

The software Ansys Mechanical 19.2 was used for the FEM simulations. Initially, static structural simulations with an unstructured TET10 mesh (Fig. 2) were performed considering the four loading cases shown in Tab. 1: only motor weight (W), only thrust (T), only torque (M), and a combination of all these loads (TMW). The adopted values were based on the weight and maximum loads shown on the motor datasheet (Turnigy 4258 Brushless). Fixed support boundary conditions were applied to the surfaces of the eight screw holes used for fixing the load cell inside the balance casing, and the loads were applied to the surface of the three screw holes used to fix the motor to the load cell (Fig. 1). The element quality distribution is shown in Fig. 3.

After the static simulations, a modal analysis was also carried out with the same mesh to evaluate the natural frequencies of the load cell, since the motor operation will cause vibrations that cannot affect the balance's reading nor its structural integrity.

Table 1. Applied loads for each simulation case. The loads are applied to the surfaces of the 3 holes used to fix the motor.

Case ID	Force (x,y,z) [N]	Moment (x,y,z) [N·m]
W	(0, 3, 0)	(0, 0, 0)
T	(0, 0, 29)	(0, 0, 0)
M	(0, 0, 0)	(0, 0, 0.7)
TMW	(0, 3, 29)	(0, 0, 0.7)

Directions x,y and z defined in Fig. 2.

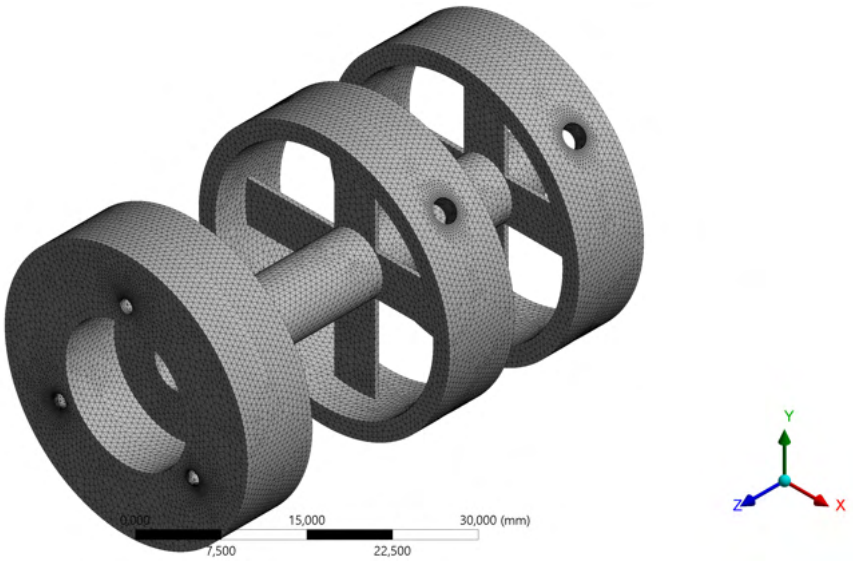

Figure 2. TET10 unstructured mesh used in the FEM simulation.

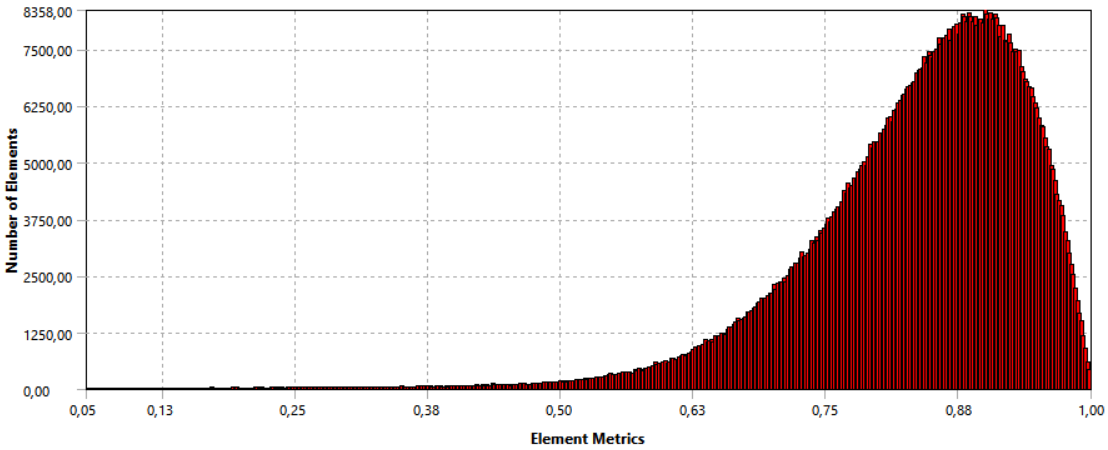

Figure 3. Element quality distribution.

4. RESULTS AND DISCUSSION

Figures 4, 5, 6 show that only load T significantly affects the strain in the x-direction of blades instrumented with linear strain gauges, responsible for measuring thrust. Thus, when subject to the TMW load expected in operation, the linear strain gauges installed at these blades will have a measurement of thrust independent of other loads (Fig. 7).

Figures 8, 9, 10 show that only load M significantly affects the shear strain in the yz-plane of the hollow shaft instrumented with a fishbone shear strain gauge, responsible for measuring torque. Thus, when subject to the TMW load expected in operation, the linear strain gauges installed at these blades will have a measurement of torque independent of other loads (Fig. 11).

The Fig. 12 shows that under maximum load, the blades of the load cell achieves a maximum von Mises equivalent stress far below the yield strength of a general aluminum alloy (280 MPa, according to the Ansys engineering data library), ensuring a safety coefficient of approximately 2.7.

For the results of the modal analysis, the natural frequency of the first vibration mode is 740 Hz, which does not represent a problem for the application considered, since the motor that will be coupled has a maximum rotation of 20000 RPM (without a propeller, with the propeller this rotation drops considerably). In this way, the operating range of the motor is far from resonating with the load cell structure.

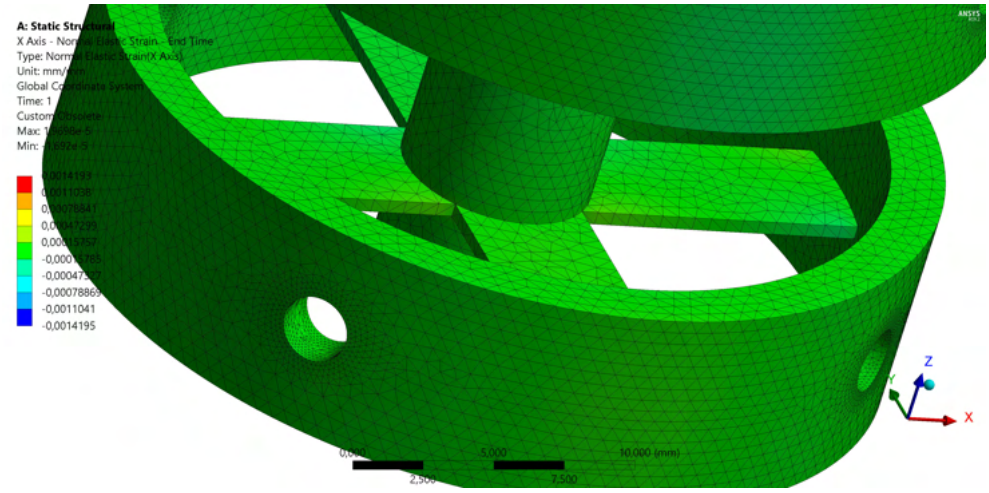

Figure 4. Case W, linear strain in the x direction.

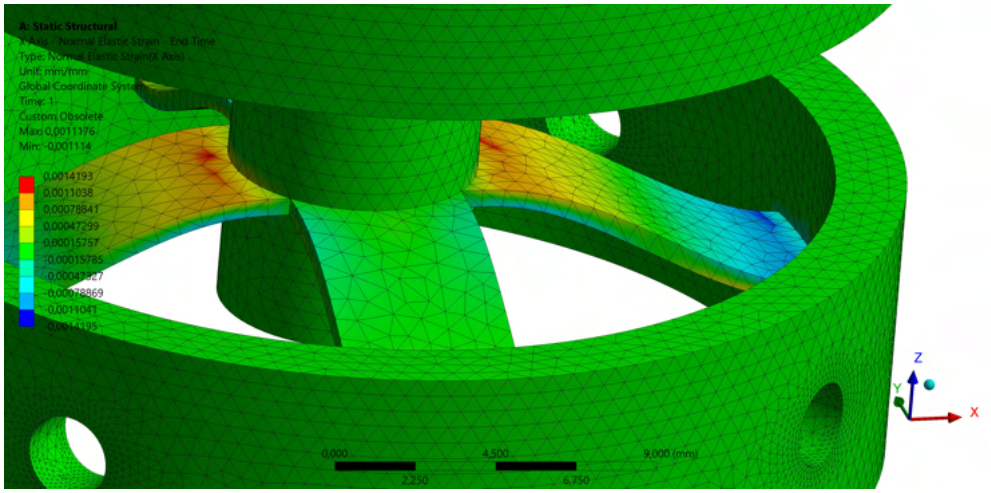

Figure 5. Case T, linear strain in the x direction.

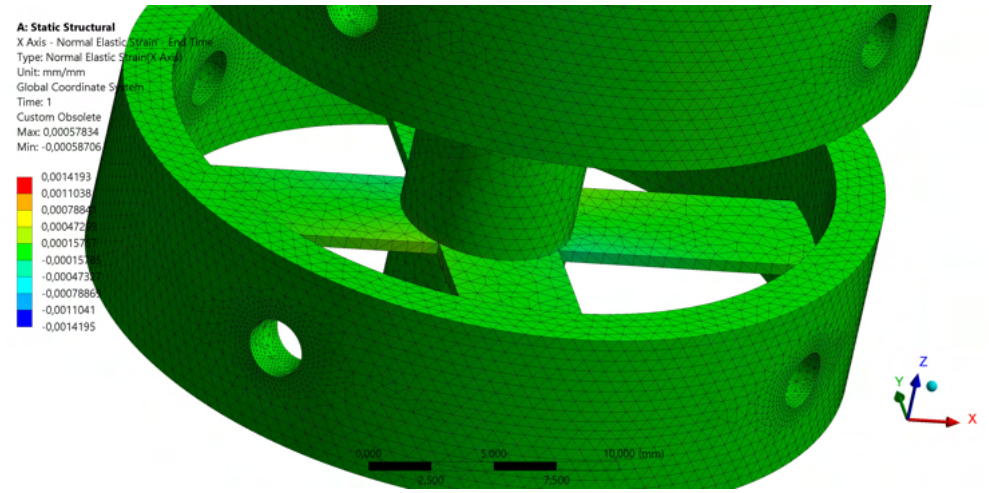

Figure 6. Case M, linear strain in the x direction, image with a deformation scale factor of 40.

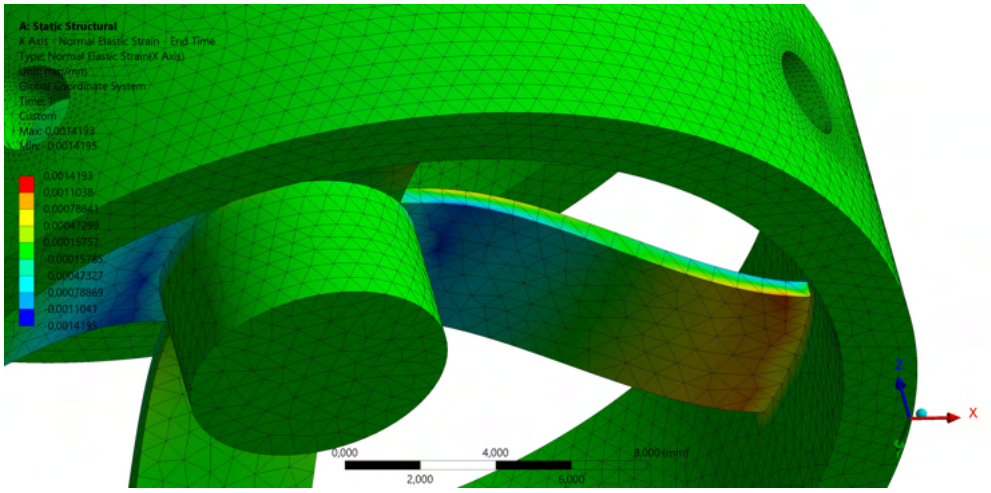

Figure 7. Case TMW, linear strain in the x direction, image with a deformation scale factor of 40.

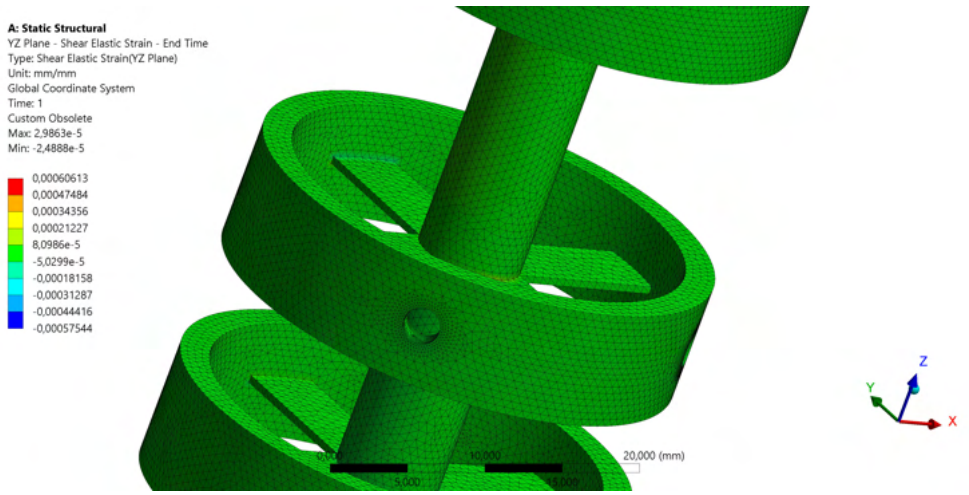

Figure 8. Case W, shear strain in the yz plane, image with a deformation scale factor of 40.

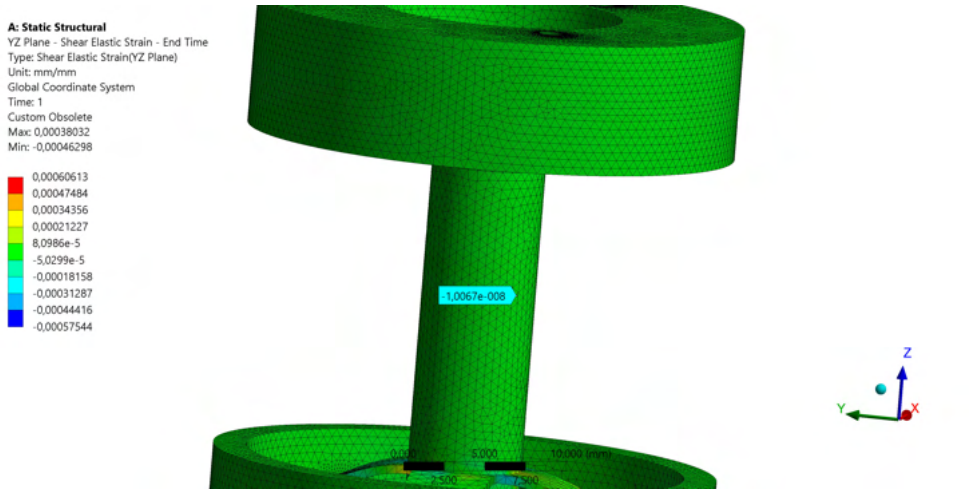

Figure 9. Case T, shear strain in the yz plane, image with a deformation scale factor of 40.

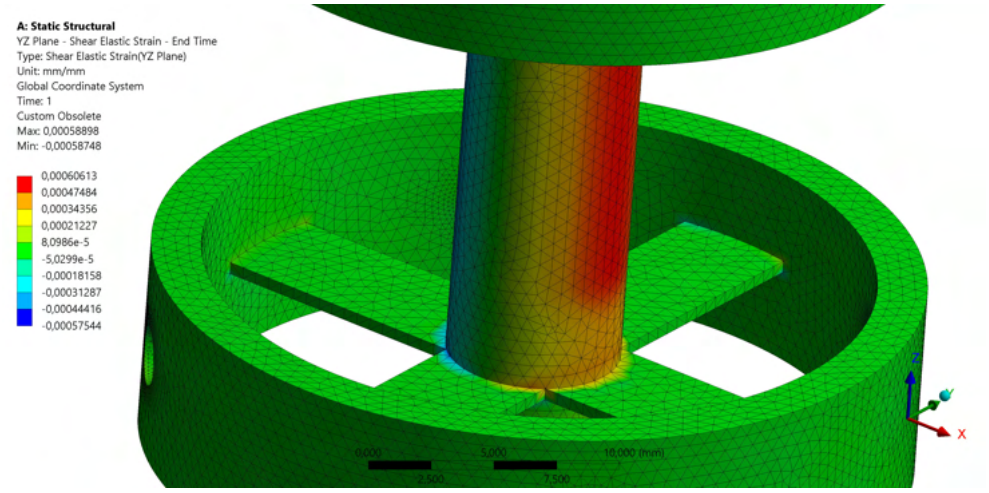

Figure 10. Case M, shear strain in the yz plane, image with a deformation scale factor of 40.

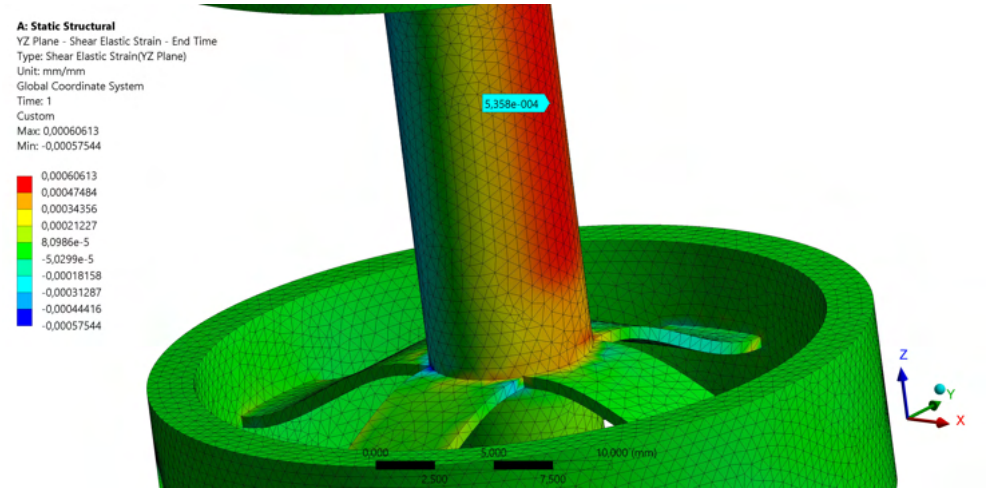

Figure 11. Case TMW, shear strain in the yz plane, image with a deformation scale factor of 40.

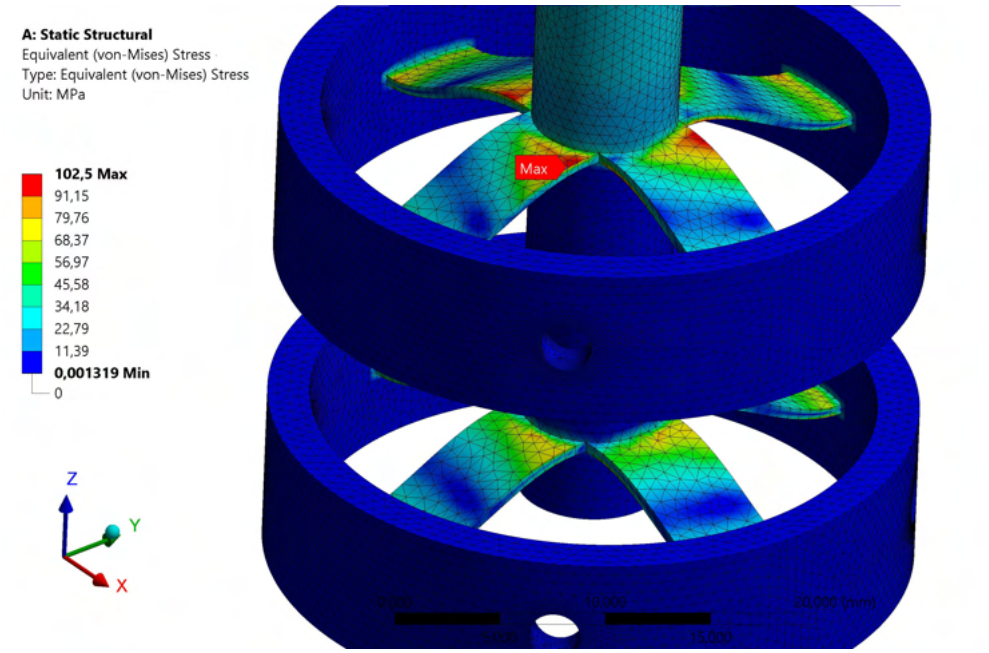

Figure 12. Case TMW, Von Mises equivalent stress, image with a deformation scale factor of 40.

5. CONCLUSION AND NEXT STEPS

The torque and thrust biaxial sensor designed was simulated using a finite element software and the results showed compliance with the requirements of independent measurements of torque and thrust. Three of these load cells were then manufactured in aluminum alloy through traditional and electrical discharge machining. The strain gauges have been installed (Fig. 13) and the balances will be soon calibrated with known loads. A measurement of the balance hysteresis will also be carried out. After the calibration process, the balances will be ready for use in the test rig.

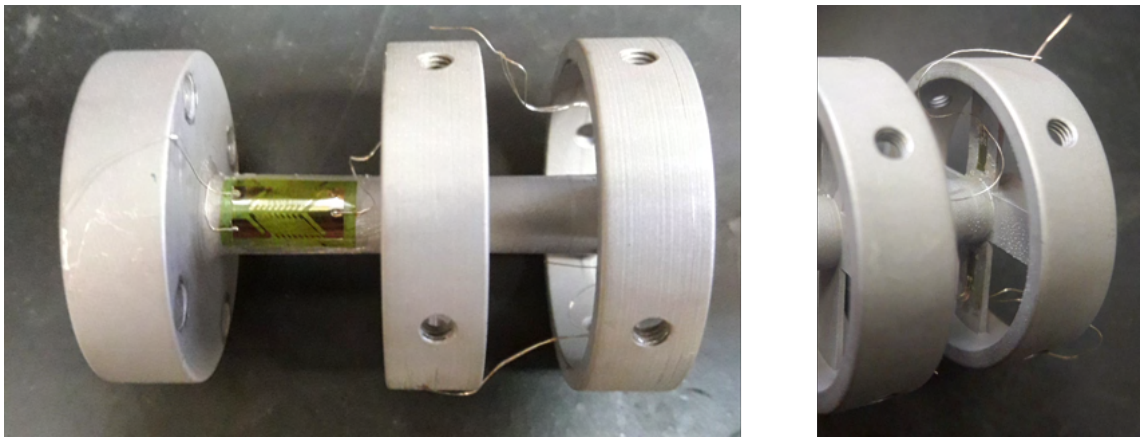

Figure 13. Strain gauges installed at the load cell.

6. FUNDING SOURCES

This work was supported by the National Council for Scientific and Technological Development (CNPq) [grant number 140352/2019-8]; the Foundation for the Enhancement of Research and Industrial Improvement (FIPAI) [grant number FB-009/19]; the Funding Authority for Studies and Projects (FINEP); and Embraer.

7. REFERENCES

Barlow, J.B., Rae, W.H. and Pope, A., 1999. *Low-speed wind tunnel testing*. John wiley & sons.

Cole, J.A., Maughmer, M.D., Kinzel, M. and Bramesfeld, G., 2019. "Higher-order free-wake method for propeller–wing systems". *Journal of Aircraft*, Vol. 56, No. 1, pp. 150–165. doi:10.2514/1.c034720.

Discetti, S. and Ianiro, A., 2017. *Experimental aerodynamics*. CRC Press.

Doebelin, E.O. and Manik, D.N., 2007. *Measurement systems: application and design*. McGraw-Hill.

International Civil Aviation Organization, 2019. "Destination green - The next chapter: ICAO environmental report 2019". Technical report, International Civial Aviation Organization.

Kim, H.D., Perry, A.T. and Ansell, P.J., 2018. "A review of distributed electric propulsion concepts for air vehicle technology". In *2018 AIAA/IEEE Electric Aircraft Technologies Symposium*. American Institute of Aeronautics and Astronautics. doi:10.2514/6.2018-4998.

8. RESPONSIBILITY NOTICE

The authors are solely responsible for the printed material included in this paper.